phys. stat. sol. (a) **184**, No. 2, 359–365 (2001)

Behavior of Stress-Induced Charges in Cement Containing Quartz Crystals

T. MATSUDA, C. YAMANAKA, and M. IKEYA

Department of Earth and Space Science, Graduate School of Science, Osaka University, 1-1 Machikaneyama, Toyonaka, Osaka 560-0043 Japan

(Received December 14, 2000; accepted January 29, 2001)

Subject classification: 77.22.Ej; 77.65.Ly; 77.84.Lf; S10

The recombination process of electric charges induced by stress release has been measured for cement samples embedded within quartz crystals to investigate the behavior of piezo-compensating charges in quartz-bearing rocks. The stress with a release constant τ of $\sigma(t) = \Delta\sigma\, e^{-t/\tau}$ led to a theoretical pulse charge density $q(t) = \alpha\,\Delta\sigma\{\varepsilon\rho/(\tau - \varepsilon\rho)\}\,(e^{-t/\tau} - e^{-t/\varepsilon\rho})$, where α, ε and ρ are the piezoelectric coefficient, permittivity and resistivity, respectively. The induced charges appeared on a sample measured with non-contacting electrodes depending on the number and orientation of synthetic quartz crystals, and two decay time constants of 0.25 and 2.5 s were obtained. The apparent piezoelectric coefficient for a sample with one piece of quartz was 1.0×10^{-15} C/N. However, the coefficients for samples with two pieces of quartz, which were arranged in the same or alternate directions, were 4.1×10^{-15} and 1.7×10^{-15} C/N, respectively. The behavior of piezo-compensating charges around quartz crystals in conductive cement suggests ferroelectric charge migration through the measurements of depolarization current.

1. Introduction

Natural granite is a composite material consisting of quartz and mica embedded in relatively conductive feldspar. Piezoelectric quartz grains in granitic rocks under static stress are electrically polarized in proportion to the stress. The polarization is quickly compensated by free charges in the conductive rock with a time constant $\varepsilon\rho$, where ε and ρ are permittivity and electric resistivity, respectively. Hence, neither the polarizations nor the free charges are detected by means of electrical measurements from outside of the rocks. The compensating charges are freed when the polarization disappears due to stress release. Such free charges can form a kind of "solid plasma" and electromagnetic waves are generated when the dipole moment disappears [1].

Temporal variations of pulsed electric potential in natural granite were studied with a compression machine [2, 3]. The electric potential decayed exponentially with a time constant ranging from 1.5 to 4.0 s [3]. The apparent piezoelectric coefficient, α_{app}, of granitic rock was two or three orders of magnitude smaller than that of quartz crystal (2.3×10^{-12} C/N).

The number, size and crystal axis of quartz grains in natural rocks are complicated [4]. Hence, electric properties have been studied in this work for 'synthetic rocks' composed of bulk cement and quartz in order to investigate the electrical properties of a composite material. A theoretical calculation was made to derive the apparent piezoelectric coefficient in a composite material and the results agreed well.

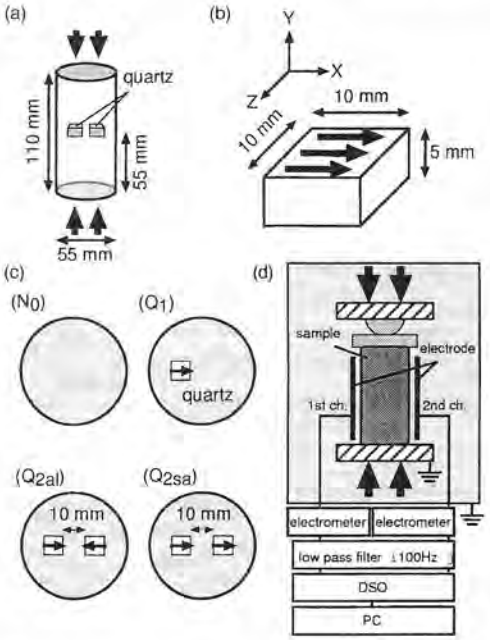

Fig. 1. a) Sample of a cylindrical cement, b) synthetic quartz and c) each sample in section. The arrows in the material denote the direction of electric polarization by Y-axis compression. d) Schematic drawing of the measurement system. Charge variation near the sample surface was measured with two non-contacting electrodes placed on both sides of the sample. The appearing charges on both electrodes were recorded in two channels of a digital storage oscilloscope (DSO) and stored into a personal computer (PC)

2. Experimental

2.1 Samples

Figure 1a shows the sample used in this study. Molds were made of polyvinyl chloride pipes with acrylic bottom plates. Standard Portland cement and water were mixed at the weight ratio of 10:3 and poured into the mold to its half height. Then, a piece of synthetic quartz single crystal was cut in blocks as shown in Fig. 1b and placed at selected positions as shown in Fig. 1c and designated as N_0, Q_1, Q_{2al} and Q_{2sa}, these contain no quartz, a piece of quartz, two pieces (with different directions) and two pieces (with same directions), respectively. After that, the rest of cement mixture was poured up to the top of the mold. One day later, the top and bottom of the samples were flattened with a file, and then stored in a dry oven at 120 °C for more than four weeks and taken out 1 h before the measurements. Cement is a material that can stand a high pressure. The resistivity of the dried cement was 2.0×10^7 Ω m.

2.2 Apparatus

Figure 1d shows a hydraulic compression machine and the measurement system of charge variation near the sample surface. The machine was surrounded with aluminum electrostatic shielding. The machine itself was grounded electrically to reduce electrical noises due to triboelectricity between the metal cylinder and the oil in the compression machine. A spherical sheet consisting of a half sphere and a dish of stainless steel was inserted between the sample and the machine to correct the angle distortion.

Two copper electrodes having width of 10 mm and height of 80 mm were placed at both sides of the sample, about 7 mm apart from the sample surfaces. The electrodes were supported by a Teflon cylinder having an inside diameter of 70 mm to avoid triboelectricity and contact electrification at their interface. The signals were measured using two digital electrometers (Advantest TR8652) with an input impedance in excess of 1×10^{13} Ω. Low-noise coaxial cables were used from the electrodes to the electrometers to reduce noise. Outputs of electrometers were recorded through low pass filters (≤100 Hz) using a digital storage oscilloscope (Yokogawa YL4100 or LeCroy 9314AM) at the sampling frequency of 100 Hz.

A strain gauge (Kyowa Electronic Instruments Co., Ltd.) was pasted on the sample N_0. The strain was measured through a strain amplifier (DPM-711B, Kyowa Electronic Instruments Co., Ltd.) and recorded with a digital storage oscilloscope. The stress was kept for a definite period of time in the range of 5 to 300 s and was unloaded in less than 1.0×10^{-1} s.

3. Results and Discussion

3.1 Strain of the samples

The variations of strain in the sample N_0 at a sudden unloading are shown in Fig. 2a for three typical stresses. The strain is proportional to the stress in the range of less than 20 MPa. The temporal variations of strain, $s(t)$ after the stress release are described as

$$s(t) = s_0 \exp\left(-\frac{t}{\tau}\right), \tag{1}$$

where s_0 is the strain before stress release and τ is the decay time constant. The decay time constants for the stress release of 4, 12 and 20 MPa were 3.3×10^{-2}, 3.2×10^{-2} and 3.3×10^{-2} s, respectively.

3.2 Time variation of the charge density

Figure 2b shows the dependence of the peak heights of polarization at stress release from 12 MPa on the stress-sustaining time for the sample Q_{2sa}. The peak heights of polarization were saturated as stress-sustaining time became longer. The result indicates the time dependent compensation for the piezoelectric polarization presumably due to the charge carrier having a low mobility. The data were fitted with an exponential saturation curve described as

$$I(t) = I_\infty \left(1 - \exp\left(-\frac{t}{\tau_c}\right)\right), \tag{2}$$

where $I(t)$, t, I_∞ and τ_c are the peak height, the stress-sustaining time, saturated peak height and a time constant, respectively. The time constant for compensation τ_c was 2.5 s in the saturation curve.

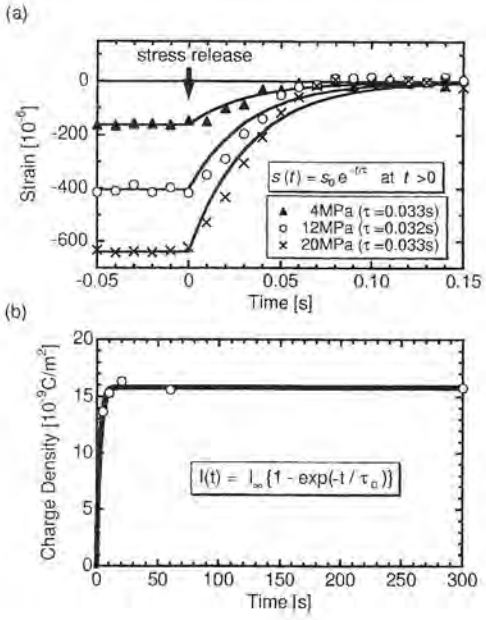

Fig. 2. a) Dependence of released stress on the temporal variation of strain for the sample N_0. The difference in the decay time is negligible for different stresses. b) Dependence of the peak heights of polarization at the stress release from 12 MPa on the stress-sustaining time for the sample Q_{2sa}

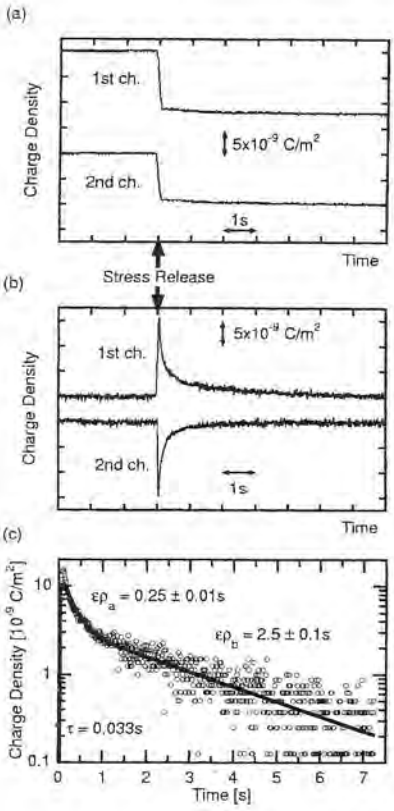

Fig. 3. Charge density variation of the first and second channels for a) sample N_0 and b) sample Q_{2sa} at abrupt release of stress from 8 MPa. c) Logarithmic plot of charge density for the sample Q_{2sa} for the first channel

The stress-sustaining time set to be 20 s in the following measurements.

Figure 3a shows the charge density variation for the sample N_0 at abrupt unloading from 8 MPa. The sample N_0 showed no attenuation of piezo-compensating charge although step-like changes were observed. The steps are likely caused by the capacitance changes which resulted from the movement of the compression machine.

The step-like changes were removed in the following experiments by using the data of the sample N_0 in Fig. 3b. The sample Q_{2sa} shows positive and negative peaks in first and second channels, respectively. This result can be considered quartz near each electrode attracted piezo-compensating charges. The signs of charge density are consistent with the direction of quartz in the samples.

Figure 3c shows the logarithmic plot of charge density variation for the sample Q_{2sa} having two pieces of quartz in the same directions with a stress drop from 8 MPa. The initial rise time of 3.3×10^{-2} s was observed as well as two decay components designated as $\varepsilon\rho_a = 0.25$ s and $\varepsilon\rho_b = 2.5$ s.

3.3 Theory of charge generation and decay

The charge density q in the electromagnetic model of geological fault [1] was described using stress $\sigma(t)$ as

$$\frac{\mathrm{d}q}{\mathrm{d}t} = -\alpha \frac{\mathrm{d}\sigma}{\mathrm{d}t} - \frac{q}{\varepsilon\rho}, \tag{3}$$

where α, ε and ρ are the charge generation constant, the permittivity and the electric resistivity of a sample, respectively. The first and second terms on the right-hand side of Eq. (3) mean the generation of charges and their decay with a time constant, $\varepsilon\rho$ in a conductive material, respectively.

As the strain variation follows Eq. (1), the stress is described as

$$\sigma(t) = \Delta\sigma \exp\left(-\frac{t}{\tau}\right), \tag{4}$$

where τ is the time constant of the stress release. Equation (3) under the condition of $q = 0$ at $t = 0$ gives a pulsed charge $\pm q$ as

$$q(t) = \alpha \Delta\sigma \frac{\varepsilon\rho}{\tau - \varepsilon\rho}\left(\exp\left(-\frac{t}{\tau}\right) - \exp\left(-\frac{t}{\varepsilon\rho}\right)\right). \tag{5}$$

The pulse shapes with the rise time of $\varepsilon\rho$ (or τ) and the decay time of τ (or $\varepsilon\rho$) for $\tau > \varepsilon\rho$ (or $\varepsilon\rho > \tau$).

The experimental decay curve was fitted using Eq. (5) considering a two-component decay process assuming $q(t) = q_a(t) + q_b(t)$ with different ρ_a and ρ_b as shown in Fig. 3c. The two components might arise from different charge carriers.

3.4 Apparent piezoelectric coefficient

Figure 4 shows the peak heights of charge density as a function of the unloaded stress for the samples Q_1, Q_{2al} and Q_{2sa}. The peak heights are proportional to stress less than 5 MPa. The apparent piezoelectric coefficient of the samples Q_1, Q_{2al} and Q_{2sa} were decided in these measurements to be 1.0×10^{-15}, 1.7×10^{-15} and 4.1×10^{-15} C/N, respectively.

The charge density induced by released piezo-compensating charges on the position of the electrode E is calculated theoretically using the method of images. Figure 5 shows the cross section of the sample and the assumed point charge positions A, B, C and D and their image charges. The charge density q_{Q1} for the sample Q_1 (considering only A and B in Fig. 5), is described as

$$q_{Q1} = \frac{1}{x_0 y_0}\frac{1}{4\pi}\sum_{i=A,B}\int_{-\frac{y_0}{2}}^{\frac{y_0}{2}}\int_{-\frac{x_0}{2}}^{\frac{x_0}{2}}\frac{q_i 2a_i}{(x^2 + y^2 + a_i^2)^{\frac{3}{2}}}\,dx\,dy \tag{6}$$

$$= 2.8 \times 10^{-8}\ \mathrm{C/m^2}\ \text{(the released stress of 4 MPa)},$$

where a_i is the distance between the electrode and each point charge and $x_0 = 1.0 \times 10^{-2}$ m, $y_0 = 8.0 \times 10^{-2}$ m, the size of electrodes. The experimental and theoretical apparent piezoelectric coefficients are shown in Table 1.

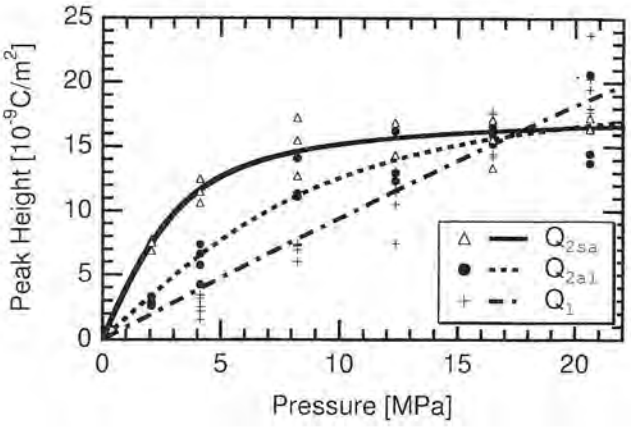

Fig. 4. Dependence of peak height on stress. The results of the samples Q_{2al} and Q_{2sa} are saturated at high stress

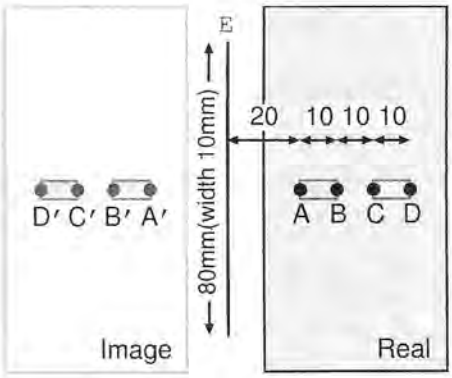

Fig. 5. Cross section of a sample including quartz and an electrode

When stress is released in the sample Q_{2sa}, the piezo-compensating charges between both quartz (B and C in Fig. 5) can approach each other and disappear faster than the other charges (A and D in Fig. 5). The higher peak appeared in Q_{2sa} suggests the possibility of ferroelectric behavior of compensatory dipolar charges.

The peak height for the sample Q_{2sa} is saturated at stress larger than 5 MPa. The result may indicate a shortage of piezo-compensating charges in a sample or a shortage of orientational polarization of water in the samples. The data are fitted with Langevin function assuming that electric field around quartz is homogeneous and proportional to the stress. The function is expressed as

$$L\left(\frac{\mu E}{kT}\right) = \coth\left(\frac{\mu E}{kT}\right) - \frac{kT}{\mu E}, \tag{7}$$

where μ, k and T are the dipole moment, Boltzmann constant and the temperature ($= 3 \times 10^2$ K), respectively.

The data of the sample Q_{2sa} was fitted with Eq. (7). From the fitting curve, $\mu E = 2.8 \times 10^{-27}\sigma$ is obtained. Actually, the electric field E in the sample is inhomogeneous. However, the electric field E_c at the center of the sample is described as $E_c = 5.5 \times 10^{-12}\sigma/(4\pi\varepsilon^*\varepsilon_0)$ considering the arrangement of quartz. While, the relative permittivity $\varepsilon^* \cong 10^4$ was obtained from $\rho = 2.0 \times 10^7$ Ω m and Section 3.2. In fact, the large permittivity was obtained experimentally at low frequency for granitic rocks [3, 5]. Hence, an extraordinary dipole moment μ larger than 5.6×10^{-22} Cm is obtained, which is much larger than that of H_2O (6.2×10^{-30} Cm). This indicates that the charges move to the edge of the sample for a distance of 1 cm about 10^8 times of one atomic distance in the above depolarization process. Hydrated water in cement will produce an extraordinary large permittivity. The extraordinary large ε^* of the

Table 1
Apparent piezoelectric coefficient of quartz-embedded cement

sample name	number of containing Qz	direction of X-axis	relative α_{app} (experiment)	relative α_{app} (calculation)
N_0	0	–	0	0
Q_1	1	–	1.0 (1.0×10^{-15} C/N)	1.0 (7.0×10^{-15}C/N)
Q_{2al}	2	opposite	1.7	0.7
Q_{2sa}	2	same	4.1	1.3

The piezoelectric coefficient of pure quartz is 2.3×10^{-12} C/N (d_{11})

order of 10^7 in natural rock might be related with the apparently low electric field intensity of 10^{-5} V/m in the earth potential measurements for earthquake prediction in geophysics.

4. Summary

Free transient electric charges induced by stress reduction were measured for 'synthetic rocks' made of cement and pieces of quartz in different arrangements. The signs of charge density in the experimental data are consistent with the direction of quartz in the samples. The obtained two decay times of the charge density may suggest two different charge carriers which compensate piezoelectric polarization. An apparent piezoelectric coefficient at less than 5 MPa of the 'synthetic rocks' containing two pieces of quartz with the same directions was about four times of that containing one piece. The orientation of electron–hole dipoles may arise from their mutual interaction among charges, which might lead to a large dipolar moment and a large permittivity ε^* at a localized area around the stress-released quartz.

Acknowledgement We would like to thank Mr. T. Kagami, Nihon Dempa Kogyo Inc. for supply of the synthetic quartz crystal.

References

[1] M. Ikeya and S. Takaki, Jpn. J. Appl. Phys. **35**, L355 (1996).
[2] S. Yoshida, P. Manjgaladze, D. Zilpimiani, M. Ohnaka, and M. Nakatani, Electromagnetic Phenomena Related to Earthquake Prediction, Eds. M. Hayakawa and Y. Fujinawa, Terrapub, Tokyo 1994 (pp. 307–322).
[3] H. Sasaoka, C. Yamanaka, and M. Ikeya, Geophys. Res. Lett. **25**, 2225 (1998).
[4] M. M. Ghomshei and T. L. Templeton, Phys. Earth Planet. Inter. **55**, 374 (1989).
[5] T. L. Chelidze, Y. Gueguen, and C. Ruffet, Geophys. J. Int. **137**, 16 (1999).